Volc. Seis., 1984, Vol. 5, pp. 97–114
0742-0483/84/0501-0097 $25.00/0

ESTIMATION OF SHEAR WAVE SCATTERING IN THE CRUST AND UPPER MANTLE OF KAMCHATKA FROM OBSERVATIONS AT THE SHIPUNSKIĬ STATION

A. A. GUSEV and B. K. LEMZIKOV

Institute of Volcanology, Far East Scientific Center, USSR Academy of Sciences, Petropavlovsk-Kamchatskiĭ

(Received January 7, 1981)

Three methods of estimating the scattering properties of the crust and upper mantle from observation of close-range earthquakes are applied to the records of the Shipunskiĭ frequency-selective seismic station located at the boundary of the main focal zone of Kamchatka. The methods employ visual examination of records for direct estimation of diffusion coefficient α, a model of low-multiplicity scattering, and diffusion model. Three series of estimates for seven octave bands with center frequencies of 0.39 to 25.0 Hz are in good agreement. The scattering length $l = \alpha^{-1}$ varies from 300 km at 0.39 Hz to 70 km at 25.0 Hz. It is shown that a significant contribution to scattering is made by multiple anisotropic scattering.

INTRODUCTION

Reliable estimates of the scattering of seismic energy in the crust and upper mantle are of great interest both as geophysical characteristics of the earth medium and as initial data in estimation of the ground motion produced by strong earthquakes. To derive estimates of scattering one has to interpret the observational data using the theory of wave scattering. This involves some difficulties.

First, one has to separate the effects of scattering and intrinsic attenuation. Second, with the existing simple theories it is difficult to take into account the effect of spatial, primarily vertical, variations of scattering and attentuation. To overcome these difficulties and to derive estimates which, though rough, are reliable, it is advisable to use several, preferably independent, methods. An attempt is made in the present paper to apply this approach to the data of near earthquakes in Kamchatka.

TECHNIQUE AND DERIVATION OF PRINCIPAL COMPUTATION FORMULAS

In this paper, interpretation of the observed wave pattern from a near earthquake is based on the simple theory of wave scattering from an impulse-type isotropic point source in a three-dimensional homogeneous attenuating earth medium with statistically uniform distribution of isotropic scatterers (see [6, 9]). Conversion scattering (P → S, S → P) and P-wave contribution to scattered wave amplitudes (coda waves) are neglected. In this case, the energy flux (intensity) of a direct wave can be written as [4, 6, 9]:

$$I_d(r) = \frac{w}{4\pi\tau r^2} \exp\left(-\frac{2\pi f r}{cQ} - \frac{r}{l}\right), \tag{1}$$

where $I_d(r)$ is the radiation intensity within a supposed frequency band Δf with center frequency f; w is the source energy in the same frequency band; r is the distance from the source to the station; τ is the duration of the pulse in the source for an assumed square pulse envelope (or an equivalent duration); $Q = Q_S(f)$ is the quality factor; $c = c_S$ is the velocity of shear waves; $l = l(f)$ is the free path or length of scattering (diffusion coefficient $\alpha = l^{-1}$). We shall rewrite (1) as

$$I_d(t_d) = \frac{w}{4\pi c^2 t_{np}^2 \tau} \exp\left(-\frac{2\pi f t_{np}}{Q} - \frac{t_d}{t^*}\right), \tag{2}$$

where $t_d = r/c$ is the traveltime of the direct wave and $t^* = l/c$ is the time of scattering.

The intensity of a scattered wave I_S can be described by different equations depending on various relationships between t_d, t^* and observation time t. Hereinafter, t is measured from the time of pulse origin, and the condition of $\tau \ll t_d$ is assumed. For $t_d \ll t \ll t^*$ the Born approximation (a single-scattering model) is valid [4, 6, 9]. It describes I_S as

$$I_1(t) = \frac{w}{2\pi c^2 t^2 t^*} \exp\left(-\frac{2\pi f t}{Q}\right). \tag{3}$$

For t close to t_d, I_S is 2–3 times greater than I_1 [4]. Practically, we can assume that $I_S = I_1$ for $t > (2–3)\, t_d$. Note that (3) is independent of t_d.

In the opposite case of $t \gg t^*$, the diffusion approximation is valid (see, for example, [9]). In this case, the scattered wave intensity is given by

$$I_d(t_d, t) = \frac{w}{c^2\left(\frac{4\pi}{3} t t^*\right)^{3/2}} \exp\left(-\frac{t^2 d}{\frac{4}{3} t t^*} - \frac{2\pi f t}{Q}\right). \tag{4}$$

Equation (4) becomes valid beginning from the times t, slightly greater than t_d. For $t \gg t_d^2/t^*$ the first term in the exponent is small, and equation (4) reduces to an asymptotic form

$$I_d(t) = \frac{w}{c^2\left(\frac{4\pi}{3} t t^*\right)^{3/2}} \exp\left(-\frac{2\pi f t}{Q}\right), \tag{5}$$

which is again independent to t_d.

No adequate analytical description is available for the $t \sim t^*$ region. Kopnichev [3] proposed an equation which structurally is a section of a $u = t/t^*$ series and which in our notation takes the form (with an error corrected in the coefficient)

$$I_{\kappa}(t) = \frac{w}{2\pi c^2 t^2 t^*}\left(1 + \frac{\pi^3}{16}u + \frac{\pi^4}{64}u^2\right)\exp\left(-\frac{2\pi f t}{Q} - \frac{t}{t^*}\right). \quad (6)$$

Figure 1 shows the curves corresponding to equations (2) (for $\tau = t^*/20$, that is fairly common in our case), (3), (4) (for three cases $t_d/t^* = 0.01$, 1, and (10), (5), and (6) (for $u < 1$). It is seen that for $u \leqslant 0.1$ equations (2) and (6) yield similar results. This

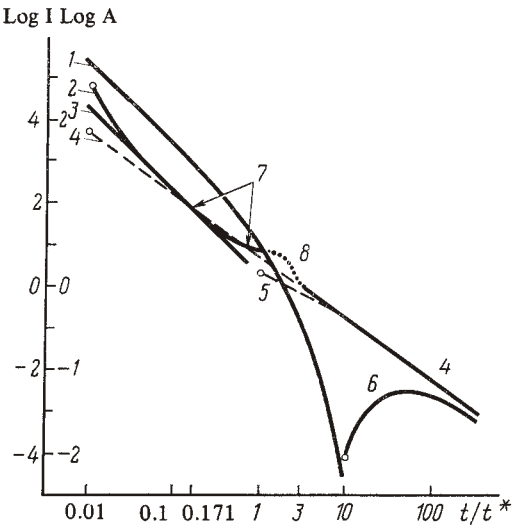

FIGURE 1 Theoretical variation of direct and scattered wave intensity as function of time from source origin. Attenuation is neglected. Ordinate is itensity. I and amplitude A in arbitrary units; abscissa is dimensionless time $u = t/t^*$, where $t^* = l/c = 1/\alpha c$. 1 direct wave for pulse duration $\tau = t^*/20$; 2 – single-scattered wave in Born approximation at distance $r = ct_d = 0.01\ ct^*$ (approximately); 3 – asymptotic variation of envelope for $t > 3t_d$ for any t_d in Born approximation; 4 – diffusion approximation for $t_d = 0.01\ t^*$; 5 – same for $t_d = t^*$; 6 – same for $t_d = 10\ t^*$; 7 – Kipnichev's model for $t < t^*$; 8 – possible extrapolation of Kopnichev's model.

can be explained by the fact that the second and third terms of the trinomial in (6) are counterbalanced by $-t/t^*$ in the exponent. For $u = 0.8$–1, equation (6) predicts a flat part of the curve; the conjugation of this flat part with the curve I_{da} (5) (for $u > 2$–3) involves a physically unreasonable peak schematically shown in Figure 1. On the other hand, the I_{da} curve (5) intersects the curve of the Born approximation (2) for $u = 0.171$, and the broken line

$$I_c(t) = \begin{cases} I_1(t); & t < 0.171t^* \\ I_d(t); & t > 0.171t^* \end{cases} \quad (7)$$

is close to the curve of (6) wherever the latter is physically plausible. For this reason we used the broken line of (7) for the interpretation. Since the actual u values fell within the 0.2–1 range, we used the second equation of (7) for I_{da} in all the cases.

A comment should be made concerning the above equations. In the case of near

earthquake energy scattering, a model of scattering in a half-space should be more adequate than infinite-space models. Analysis of this case shows, however, that if the half-space boundary is assumed to be a mirror surface, the use of equations (3) and (5) does not involve any appreciable errors.

Equation (7) describes an extreme theoretical variation (in the case of large t values) of scattered wave intensity for any t_d in a statistically homogeneous medium with constant intrinsic attenuation. As evidenced by the observational data, this extreme variation (a "coda-wave asymptote" in [7]), i.e., an extreme shape of the envelopes in the tail of the near earthquake record at different distances from the source, is a common feature of the wave pattern. The empirical dependence I_s (t), however, cannot be described by an equation of the (7) type; it must be expressed by a more complex equation because the condition of statistical homogeneity and constant attenuation is not satisfied. Consequently, the use of the above theoretical models for the interpretation needs further substantiation.

It is well known that in the earth scattering generally decreases with depth. Let us, then, consider a simple heterogeneous model consisting of a scattering layer with $t^* = t_1^*$ having a thickness $H \ll ct_1^*$ lying on a weakly scattering half space with $t^* = t_2^*$. We shall denote $t_h = (Ht_1^*/c)^{0.5}$ and assume the medium to be perfectly elastic. It is evident that for $t \ll t_h$ the wave field observed at the earth's surface will correspond to scattering in a half space with t_1^*. It is less evident that for $t \gg t_h$ the wave field will conform to scattering in a half space with t_2^*. For intermediate t values the wave field will correspond to scattering in an *attenuating* half space with a characteristic "attenuation time" $t_Q = Q/2\pi f$ in the order of t_h and an effective value of $t^* = t_e^*$. Fictitious attenuation arises because of an essentially irrevocable energy loss by radiation into a weakly scattering medium. Thus, some fictitious attenuation will be added to the layer's attenuation when it is estimated using the diffusion model in an attenuating half space.

Some conclusions concerning the interpretation follow from the above consideration. First, one should try to estimate t* independently of Q. Second, for adequate interpretation using the diffusion model in a homogeneous half space it is necessary that the experimental data fit the model within a sufficiently broad range of t. Finally, it should be expected that the Q values estimated by the half-space diffusion model will be somewhat underestimated, and the more narrow the t range, the greater the underestimation. Generally speaking, an inverse, apparently unstable and ambiguous, problem of reconstructing t* (h) and Q (h) from intensity variation I_s (t) can be formulated; investigation of this possibility is a matter of the future.

Another factor complicating the real situation, as compared with the above-mentioned model, is the fact that the hypothesis of isotropic scattering, on which the equations of the Born and, to a lesser extent, diffusion approximations are based, does not hold in the real earth. This is manifested, in particular, by the fact that on short-period records of regional stations a direct wave, i.e., a pulse generated in the source, can be observed only at distances of not more than 10–20 km from the source. At greater distances it becomes broader, and its duration does not represent that in the source. Isotropic scattering does not predict broadening of the pulse. In this connection it is worth mentioning that one of the most common scatterers in the earth is a reflector, well known in seismic exploration and in deep seismic sounding; scattering properties of this reflector are highly anisotropic.

An attempt is made below to approximate the combination of isotropic and highly anisotropic scattering. The total diffusion coefficient α, in this case, is a sum of isotropic α_i and anisotropic α_a coefficients.

$$\alpha = \alpha_i + \alpha_a. \tag{8}$$

We shall now introduce the scattering distances $l = \alpha^{-1}$, $l_i = \alpha_i^{-1}$, $l_a = \alpha_a^{-1}$, the times $t_i^* = l_i/c$ and $t_a^* = l_a/c$, and the densities of the scatterers n_i and n_a. The integral scattering cross-sections are

$$\sigma_i = \alpha_i/n_i, \tag{9}$$

$$\sigma_a = \alpha_a/n_a. \tag{10}$$

The differential cross-section of isotropic scattering is constant

$$\sigma_i(\theta) = \sigma_i/4\pi. \tag{11}$$

where θ is the scattering angle. For anisotropic scattering the scattering angle θ is assumed to be small; in this case, the small arc θ on a unit sphere is a vector sum of two small arcs, θ_X and θ_Y, which are the angular ray deflections in two mutually perpendicular directions. The random scattering angle is then given by

$$\theta = (\theta_x^2 + \theta_y^2)^{1/2}, \tag{12}$$

where θ_X and θ_Y are independent random quantities. Let θ_X and θ_Y obey the same normal distribution law with variance δ^2 ($\delta \ll 1$):

$$p(\theta_{x,y}) = (1/\delta\sqrt{2\pi}) \exp(-\theta_{x,y}^2/2\delta^2). \tag{13}$$

In this case, θ has a Rayleigh distribution, and a differential anisotropic scattering cross-section has the form

$$\sigma_a(\theta) = (\sigma_a\theta/2\pi\delta^2) \exp(-\theta^2/2\delta^2). \tag{14}$$

We now proceed to consider multiple anisotropic scattering. By following the ray direction in the course of multiple scattering we can assume the scattering process to be random wandering in a space of angles (over a single sphere). This process has been considered in [8, p. 139], and we shall borrow the relevant results.

Let θ be the total angle of the ray deflection for N scattering acts; the mean $\cos\theta$ is in our notation

$$\overline{\cos\theta} = e^{-N\delta^2}. \tag{15}$$

For a small value of the exponent, equation (15) reduces to

$$\overline{\theta^2} = 2N\delta^2. \tag{16}$$

As N increases, $\cos\theta \to 0$, the radiation field becomes progressively isotropic. We then select $N\delta^2 = 2$ as a provisional critical value which corresponds roughly to $\theta = 82°$, and refer to the respective time $t_0 = 2t_a^*/\delta^2$ as the time of isotropization. For $t > t_0$ the scattered field will differ little in character from the case of isotropic scattering at $t^* = t_0$. On the other hand, for $t \ll t_0$, when anisotropically scattered energy propagates

along the initial ray, the main effect will be the broadening of a radiated pulse with the energy being preserved at approximately the same level. Thus, we can assume that at $t \ll t_0$ the energy of the observed pulse is close to the energy of a pulse in a medium free of scattering. This is important for the interpretation because usually it is difficult to observe a "pure" pulse from a source.

The above consideration applies to the anisotropic part of scattering. The isotropic part for $t \ll t_i^*$ merely entails the pulse amplitude decay. If the conditions of $t > t_0$ and $t > t_i$ are satisfied at the same time, the effects of the isotropic and anisotropic parts are indistinguishable, and the situation assumes the character of multiple isotropic scattering with some effective α_e and t_e^* values:

$$\alpha_e = \alpha_i + (t_a^*/t_0)\,\alpha_a,$$

$$t_e^* = (c\alpha_e)^{-1}. \tag{17}$$

Some of the anistropic scattering parameters can be estimated from the broadening of the pulse. Indeed, it can be assumed that with a δ-shape source pulse the pulse duration will be on the order of a difference between the traveltime along the straight ray in a homogeneous medium and the traveltime along the "curved" ray in a scattering medium. According to [8], for $N\delta^2 \ll 1$ the mean square distance r^2 of the ray from the initial point while the scattered wave travels the distance $s = Nt_a^*$ is given by

$$r^2 = s^2\left(1 - \frac{N\delta^2}{3}\right) \tag{18}$$

which gives

$$s - r \approx N\delta^2 s/6 = t^2\delta^2/6t_a^* c$$

and the pulse duration

$$\tau \approx \delta^2 t^2/6t_a^* = qt^2. \tag{19}$$

The q parameter and $t_0 = \frac{1}{3}\,q$ can be determined from observation. The value of t_a^* cannot be determined directly, but assuming δ from a permissible range (roughly $10^\circ < \delta < 30^\circ$) we can have an approximate t_a^* estimate from

$$t_a^* = t_0\delta^2/2. \tag{20}$$

The relative effect of multiple anisotropic scattering in total scattering can be estimated by comparing the t_0 and t_e^* values determined from coda wave observation.

The list of possible departures of the real earth medium from the model of isotropic scattering in a statistically homogeneous medium could be continued. We believe, however, that vertical heterogeneity and anisotropy are the most important.

METHOD OF INTERPRETATION

We have mentioned above that for the estimation of α (or $1 = \alpha^{-1}$, or $t^* = 1/c$) it is advisable to use methods that do not involve the simultaneous estimation of intrinsic attenuation. For instance, it is convenient to use waves of two types, direct and scattered, at

the same delay time Δt. The most approximate method we used is based on visual examination of seismograms and on estimating the possibility of identifying a direct (or anisotropically scattered) wave. When these estimates of the quality of a "direct wave" are arranged over the distance, we can find the critical time t at which the direct wave is "lost in noise". This time can be used as a direct estimate of t*.

The validity of this method can be substantiated by the following. Wave patterns recorded from near earthquakes point to a great effect of anisotropic scattering because a direct wave (a source pulse) cannot be visually identified even at the smallest distances. If the isotropic constituent of scattering is neglected, the time, at which the visible pulse of an anisotropically scattered wave is "lost", will be slightly smaller than the time of isotropization, which in this case is close to scattering time t*. Hence, this estimate is reasonable.

Consider now the opposite case, where scattering is essentially istropic. Here, the "pulse loss" occurs at the time when the intensities of a direct and a scattered wave are identical. But, as we have mentioned above, the pulse of a direct wave is broadened, and, consequently, its actual rather than "focal" length should be used during the evaluation of the direct wave intensity. At low frequencies the pulse is broadened by filtering at the frequency-selective seismic station (FSSS) rather than by multiple anisotropic scattering. The actual pulse widths are usually $\tau = 1.5$–8c.

Assuming that the "pulse loss" occurs at some definite signal-to-noise ratio $\gamma \sim 1$, we obtain the equation from which the time of "loss" can be estimated

$$I_d(t')/I_s \quad (t') = \gamma, \tag{21}$$

where I_d is derived from (2) and I_s from (7). I_s corresponds to $t \sim t_d$, and in this case equation (7) is, strictly speaking, inapplicable. For a rough estimation, however, its application seems permissible. The fact is that at $t \sim t_d \ll t^*$ equation (7) underestimates and at $t \sim t_d \gg t^*$ overestimates I_s; but we deal with the boundary case of $t \sim t_d \sim t^*$. Solving equation (21) for $I_s = I_c$ (equation 7), we obtain $\gamma \sim 1$ for $t' \sim t^*$, if we substitute the most common τ' values and the t^* estimates obtained below by different means. This fact and the result obtained for the purely anisotropic case justify the proposed rough approach. It should be mentioned that when using this approach one should carefully avoid any preliminary selection of records.

The second method we used to estimate t* is based on the ratio of direct wave intensity to that of a scattered wave (of low multiplicity) for different earthquakes. We shall write equation (7) for one earthquake (index 1) and equation (2) for the other (index 2) and take a ratio of the right-hand and left-hand sides assuming t to be identical. Dividing the result by w_1/w_2 we obtain the equation

$$B_2 \equiv \frac{I^{(1)}_s w^{(2)}}{\tau^{(2)}_e I^{(2)}_d w^{(1)}} = \begin{cases} (2/t^*) \exp(t/t^*); & u < 0.171 \\ (4{,}836/t^*)(t/t^*)^{1/2} \exp(t/t^*); & u > 0.171 \end{cases}, \tag{22}$$

where τ_e is the equivalent pulse duration. Given t and B_2, we obtain an equation for t* which can be solved, for instance, by the method of iteration. The choice of t is governed by the following considerations. The $t/t_d(1)$ ratio should be maximum to permit the application of the asymptotic equation; on the other hand, t must be minimum so that the parameter u should not be greater (for $u \geqslant 1$ the estimation of I_d (2) is unstable).

We now proceed to B_2 estimation and begin it with a simplified case where I_s and I_d

are fixed for one and the same earthquake (in this case $B_2 = I_S/\tau_e I_d$). In this work we used photopaper records; our initial data were the peak-to-peak direct wave amplitudes $2A_S$ with the respective visually estimated pulse lengths τ' and the peak-to-peak coda amplitudes $2A_C$ at the reference time intervals Δt. We shall first consider the $\tau_e I_d$ estimate. By definition. $\tau_e I_d = \tau_e\, c\rho A^2_{rms}\, M^2$, ρ is density, M is magnification, and A_{rms} is the mean square amplitude of the record of the equivalent pulse. Since the multiplier $C = c\rho M^2$ is eliminated from (22) by division, it is sufficient to estimate the product $\tau_e A^2_{rms}$.

The true "source" τ_e value is usually hard to determine, but what is important for us is the pulse energy. It is, hence, convenient to adjust the observed results to the reference level equal to the equivalent length of the filter response $\tau_f\ \mu\ \Delta f^{-1}$. We then relate the A_{rms} value to the observed A_S and τ' values

$$A_{\text{increase}} = k_\tau k_1 k_2 k_3 k_4 A_S, \tag{23}$$

where $k\tau$, k_1, k_2, k_3, k_4 are the correction factors whose estimation is made by the following procedure.

We shall first consider the correction for pulse duration. The bandpass filter response of the frequency-selective seismic station (FSSS) with center frequency f_m and frequency band $\Delta f = 0.67 f_m$ has an equivalent duration $\tau_f = 1.5 f_m^{-1}$. The observed visible length of the filter response τ_0 (at the amplitude level of ~ 0.2) is close to $2\tau_f$. The observed length of the S-wave pulse is commonly greater than τ_0, especially at high frequencies. This could be due to the effect of the source pulse duration or to anisotropic scattering. In the former case the length must be identical at different channels. Inasmuch as identity was observed in very rare cases, we attributed this effect to anisotropic scattering. Since in the case of anisotropic scattering the energy is, on the average, preserved, the observational data can be adjusted to the reference length; it is convenient to adjust them to τ_0. The respective correction factor for A_S is

$$k_\tau = (\tau'/\tau_0)^{1/2}, \tag{24}$$

where τ_0 like τ', is read off at the amplitude level of ~ 0.2. The adjusted amplitude is given by

$$A_0 = k_\tau A_S. \tag{25}$$

To pass from A_0 to A_{rms} the following correction factors should be used.

1. Correction for the transition from the visible length of the filter response τ_0 to τ_f:

$$k_1 = (\tau_0/\tau_\phi)^{1/2} = 1.41. \tag{26}$$

2. Correction for the transition from the smooth envelope of the filter response to the square envelope. We assume that the envelope is described by a sinusoid half-wave; the correction, in this case, is

$$k_2 \approx 0.707. \tag{27}$$

Corrections k_1 and k_2 practically counterbalance each other.

3. Correction for the transition from the maximum extremum to the rms extremum.

This correction is estimated as follows. The largest part of the transient pulse of the direct wave, with a length of around 0.4 τ, is regarded to Gaussian noise. Then the squared extrema are exponentially distributed and (see [2])

$$k_3^{-2} = \sum_{i=1}^{n} 1/i \approx \ln n + 0.577, \tag{28}$$

where the number of extrema n = 0.4 τf_m. A_s is actually a half-sum of two maximum extrema of n peaks and n troughs. This does not effect the correction but decreases the scatter of estimates.

4. Correction for the transition from the rms extremum to the rms amplitude. As in the case of a Gaussian process, we assume

$$k_4^2 = 0.5. \tag{29}$$

The estimation of $I_S = CA_{rms}^2$ with respect to A_C is somewhat simpler. Since $2A_C$ is a peak-to-peak amplitude within a fixed window Δt, we have

$$A_{\text{increase}} = k_3'(\Delta t)\, k_4' A_C, \tag{30}$$

where k_3' and k_4' are similar to the above mentioned corrections k_3 and k_4, and k_4' = k_4. Thus our simplified problem (for one earthquake) is solved.

Actually, we dealt with records of many earthquakes obtained at one station. It is, then, desirable to find a method of averaging data from different earthquakes. For this purpose, it is convenient to normalize A_0 and A_C values by A_C values for some sufficiently large reference time t = t_r [7]. Since $A_C^2(t_r)$ is proportional to w, this approach agrees perfectly with the initial equation (22). The normalized values

$$a_S = A_0(t)/A_c(t_r), \tag{31}$$

$$a_C = A_C(t)/A_c(t_r) \tag{32}$$

must on the average be independent of the choice of a particular earthquake. Since, however, the actual a_C and, especially, a_S estimates exhibit a great scatter, it is convenient to average the relationships $\bar{a}_S$ (t) and $\bar{a}_C$ (t) for several earthquake, and to use the averaged $\bar{a}_S$ and $\bar{a}_C$ values to calculate B_2 for some fixed t value. .

In the $\bar{a}_S$ calculation, we could not always measure A_C (t_r). In such cases, we performed a normalization procedure using the explicit equation (see [7]).

$$a_S = (A_0(t)/A_c(t'))\,\bar{a}_c(t'), \tag{33}$$

where t' is a different time which is convenient for measuring amplitude.

The a_S calculation can be made only for some of the recorded earthquakes, namely, those whose durations τ' can be measured with certainty. Hence, the average empirical values are upward biased because the data corresponding to low values of a radiation pattern and to the paths where scattering is essentially higher than the average are automatically eliminated. To avoid this bias we used one more correction factor, $k_2^5 = 0.8$, in all the calculations which involved $\bar{a}_S$.

Since the k_3 value depends, though not greatly, on τ', in calculating B_2 we used a median τ' value which is equal to τ_m. We now can write the final formula

$$B_2 = k_{C/S}^2 (\bar{a}_C(t)/\bar{a}_S(t))^2 \, 0{,}67 f_m, \tag{34}$$

where

$$k_{C/S} = k_3'(\Delta t)/k_3(\tau_m)\, k_5. \tag{35}$$

The third method we used to estimate t* was based on the diffusion model. In this case, we could not avoid estimating Q. The general-procedure of the method is as follows. The first step is to check if the empirical curves $\bar{a}_C$ (t) can be adjusted by the equation (derived as a consequence from (4), see [7, 9]).

$$f(t) = \text{const}\, t^{-3/4} \exp(-\pi f_m t/Q). \tag{36}$$

Q is estimated during the adjustment. The next step, as in the second method, is to divide both sides of (7) by both sides of (2) for different t values which can be given as t_d and t_s, respectively. We obtain.

$$B_3 \equiv \frac{I^{(1)}{}_s(t_s)}{I_d^{(2)}(t_d)\,\tau_e^{(2)}} = \frac{4{,}836 t_d^2 \exp((t_d - t_s)\, 2\pi f_m/Q + t_d/t^*)}{(t^* t_s)^{3/2}}. \tag{37}$$

With the known values of B_3, t_d, t_s, f_m, and Q we obtain the equation from which t* can be estimated. B_3 is found from the equation which is similar to the one we used to estimate B_2

$$B_3 = (k_{C/S})^2 (\bar{a}_S(t_d)/\bar{a}_C(t_s))^2 0.67\, f_m. \tag{38}$$

Here the minimum possible t_d value is selected, and t_s is taken from the end of the t range where the a_C (t) adjustment by the (36) function is feasible.

We shall now consider the procedure of estimating parameter q (equation (19)) which determines are characteristics of anisotropic scattering. To apply the approach evolved above to the observational data, we should take into account the duration of the response pulse of the FSSS channel. The observed pulse duration can be, in this case, written in the form

$$\tau' = (\tau_0^2 + (qt^2)^2)^{1/2}, \tag{39}$$

where τ_0 is the FSSS response pulse duration. This equation is exact if the rms durations are assumed for τ', τ_0 and qt^2:

$$\tau = \int \varphi^2(t)\, t^2 dt / \int \varphi^2(t)\, dt, \tag{40}$$

where φ^2 (t) is the square envelope. It would be advisable to consider a similar correction to allow for the pulse duration in the source but it is small enough to be neglected. Equation (39) can be directly adjusted to the observational data on τ'.

OBSERVED DATA AND SCATTERING ESTIMATES

In this work we employed several dozen records of the Shipunsky multichannel frequency-selective seismic station, located on the east coast of Kamchatka (tip of Cape Shipunsky, 100 km east of Petropavlovsk-Kamchatskiĭ). The station, designed by K. K. Zapol'skiĭ, was operated from 1967 to 1969 by S. A. Boldyrev [1]. The station's seven octave channels recorded vertical ground motion at center frequencies f_m = 0.39, 0.79, 1.51, 3.0, 5.5, 11.1, and 25.0 Hz in the equivalent band of around 0.67 f_m. The station located on hard rock recorded near shallow earthquakes with an S-P time interval of 5–40 s; it was virtually unable to record earthquakes with smaller S–P intervals. It was assumed in the calculation that $c = c_s = 3.5$ km/s $(c_p/c_s)^2 = 3.0$.

First we examined the unpreselected records for the "quality" of the S-wave pulse. We limited our sample of records to 35 records which were known with certainty not to have been preselected. We used three levels of visual classification of a pulse quality, "explicit", "poor", and "unidentifiable", that were marked by number 1, 2, and 3, respectively. The average mark was calculated for each S–P interval out of the set of 5–10, 10–20, 20–40, and 40–80 s intervals, and the S–P value corresponding to the average mark of 2.5 was adopted as a value characterizing the length of scattering (see Figure 2). The t* values estimated by the first (visual) method are listed in Table 1.

TABLE I

Estimation of t* by First (Visual) Method

Parameter	Center frequency f_m, Hz						
	0.39	0.74	1.51	2.96	5.5	11.1	25.0
$(S-P)_{2.5}$, s	34	23	23	23	17	7	(5)
t*, s	80	54	54	54	40	17	(12)

Then, using a few dozen earthquakes, we plotted the asymptotic coda-wave envelopes $\bar{a}_c(t) = \bar{A}_c(t)/\bar{A}_c(100)$ normalized by their own level at t = 100s. According to [7], the "onset" of the coda-wave record was selected at t = 1.5–2.5 t_d (a smaller t was used for high-frequency channels). Like in the other regions of the USSR [7], we found the coda-wave envelopes to be stable for different event locations. The method of plotting the asymptote was borrowed from [7] with some modification which we had proposed earlier [2]. The coda-wave record was broken into intervals of equal duration Δt with the interval boundaries chosen at $t_i = i\Delta t$, i = 1, 2, ... (as in the previous case, t was measured from the event origin). The Δt values are listed in Table 3. The peak to peak coda amplitude $2A_c(i)$ was measured at each interval, and the log $A_c(i)$ sets for different earthquakes were plotted. Displacing separate curves along the vertical, we plotted the resulting curve $\bar{a}_c(t)$.

For Q estimation we adjusted the $\bar{a}_c(t)$ curves by function (36) in the left-hand initial part of the graph (Figure 3). The results are given in Table II, where line $t_a - t_b$ indicates the interval over which the adjustment is virtually perfect, with a discrepancy of less than 0.05 log units. For $t > t_b$ the empirical curves depart smoothly upwards from the theoretical ones.

To plot the $\bar{a}_s(t)$ relationship we selected records with easily recognizable S-wave

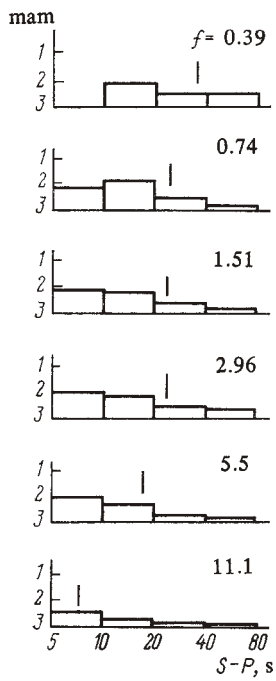

Figure 2

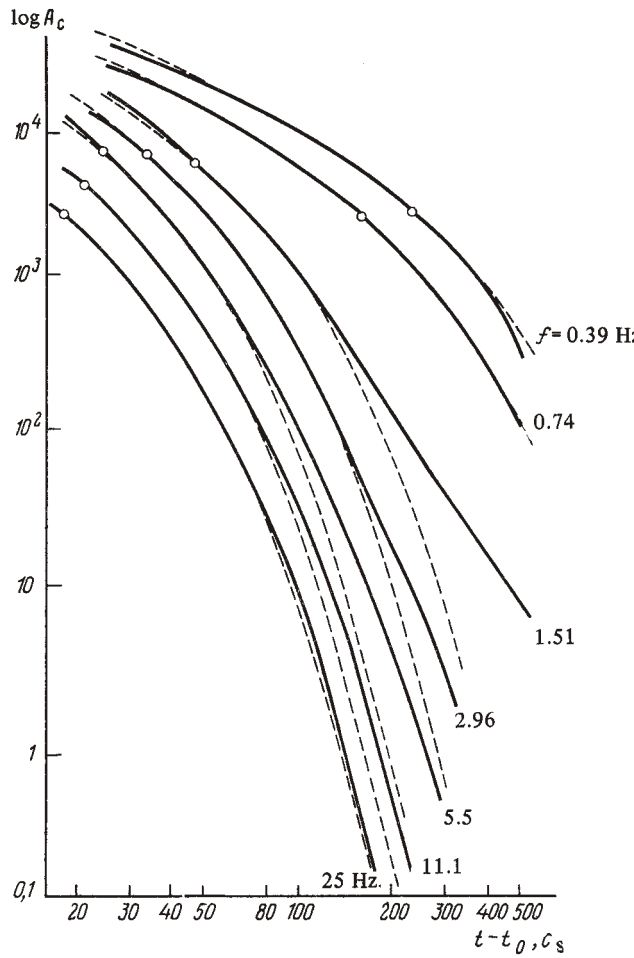

Figure 3

FIGURE 2 Variation of medium-quality direct wave in marks as function of S-P interval (see text) for six FSSS channels. Vertical mark shows time of pulse loss in noise.

FIGURE 3 Empirical asymptotic envelopes of coda-wave amplitudes a_C (t) for seven FSSS channels and their approximation by theoretical curves for diffusion model. Center filter frequencies are indicated at curves. Curves are arbitrarily shifted along vertical; points indicate time $t = t_Q$.

pulses. For these pulses we measured peak-to-peak amplitudes $2A_S$ and visually read off duration τ' at the 0.1--0.3 amplitude level. For each record we calculated the adjusted amplitude A_0 and normalized it by A_C (100) of the same record following the above-mentioned procedure. The a_S values are shown in Figure 4 as a function of t_d. The scatter is great, and the slope of the averaging curves can hardly be estimated. In order to evaluate the level of the averaging curves, we plotted theoretical curves of the form

$$a(t) = \text{const.}\ t^{-1} \exp(-\pi f_m t/Q - t/t^*)$$

(41)

The Q values were chosen from Table II, and the results of the preliminary calculation, close to the final ones, were adopted as t* values. The estimation of the levels of the curves is not affected by large variations of t* making this procedure permissible. The levels of the curves were chosen visually (see Figure 2). The levels of the selected curves were used as $\overline{a}_S$ (t) in further calculation.

The choice of $t = t_2$ in the second procedure was constrained to a narrow range where the relationships $\overline{a}_C$ (t) and $\overline{a}_S$ (t) overlapped. We selected t_2 = 25 s for three low-frequency channels and t_2 = 20 s for high-frequency channels. In the case of the $\overline{a}_C$ data, parameter t/t_d was 2.0 and 1.6, respectively. Parameter B was calculated as above; the results are listed in Table III. The $u = t_2/t^*$ values are given in the last line of the table. It is seen that $u > 0.171$ everywhere and, hence, the second equation of (22) was used in all cases.

In the calcuation by the third method, the minimum value, 14 s, was taken for the direct-wave time $t_{3,\,d}$, and the value close to t_b from Table II for the scattered-wave time $t_{3,s}$. The results calculated by this method are listed in Table IV.

In order to obtain the characteristics of anisotropic scattering, we adjusted the τ (S–P) data for three FSSS channels (1.51, 2.96, and 5.5 Hz). Figure 5 shows the initial data and the averaging curves

TABLE II

Estimation of Q_S from Coda Waves by Diffusion Model

Parameter	Center frequency f_m, Hz						
	0.39	0.74	1.51	2.96	5.5	11.1	25.0
t_a–t_b	30–500	25–500	25–130	25–180	20–80	20–80	20–180
Q_S	298	367	227	307	414	722	1445

TABLE III

Estimation of t* by Second Method

Parameter	Center frequency f_m, Hz						
	0.39	0.74	1.51	2.96	5.5	11.1	25.0
τm, s	8	4	2.9	2.5	2.55	2.3	2.2
Δt, s	10	10	10	5	5	5	2.5
log $K_{S/C}$	−0.04	−0.10	−0.10	−0.03	+0.01	−0.02	+0.04
t_2, s	25	25	25	20	20	20	20
log $\overline{a}_S$	0.95	0.70	1.41	2.28	2.71	2.87	3.18
log $\overline{a}_C$	0.5	0.64	1.13	1.58	1.94	2.10	2.39
t*, s	89	33	37	52	40	30	24
u	0.26	0.60	0.58	0.36	0.48	0.78	1.05

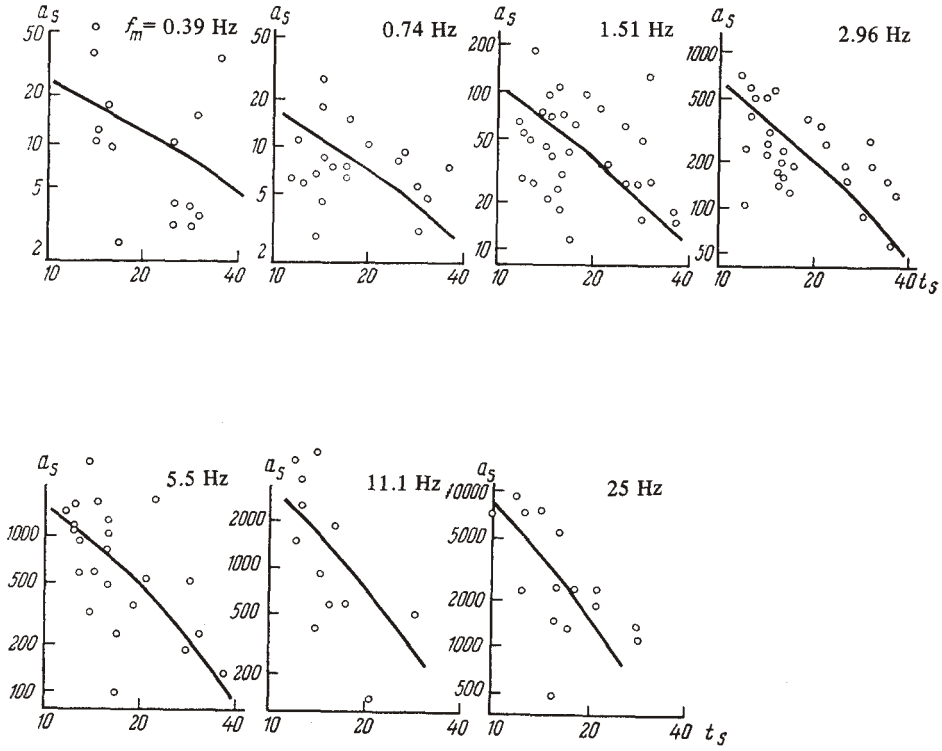

FIGURE 4 Empirical a_S (t) values for seven FSSS channels and averaging curves (see text).

$$\tau' = (\tau_0^2 + p^2 (S - P)^4)^{1/2}. \tag{42}$$

(see equation 39), where τ' and τ_0 are the length of the observed pulse at the output of the FSSS channel and the duration of the FSSS response pulse at the amplitude level of 0.2; p is the adjustment parameter; $\tau_0 = 2/0.67\ f_m$.

The quality of adjustment was, in our opinion, satisfactory; the scatter was great, but this should probably have been expected. The best results were obtained at the 5.5 Hz channel, where the theoretical mean square relationship can be considered to be confirmed. The values of q = 0.178 p and the calculated t_0 values are given in Table V.

For a rough estimation the scattering chart width δ was assumed to be 20°; the respective t* value is also given in Table V. To judge the validity of these estimates, we divided the t_a^* values by the wave period $T = f_m^{-1}$; the result is a dimensionless "scattering number" Λ_a, equal to the number of wavelength λ over the scattering (free path)

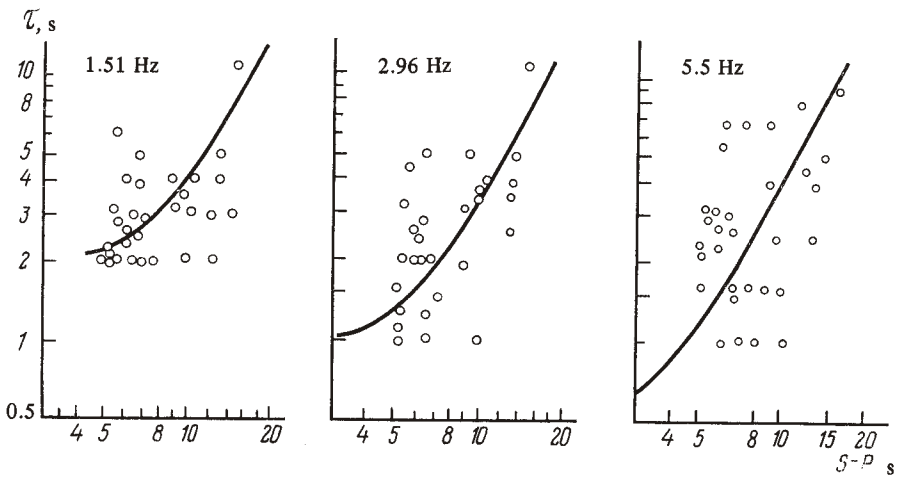

FIGURE 5 Variation of visual duration of "direct" S-wave t three FSSS channels with distance. Curves correspond to equation (43); parameter p was adjusted.

TABLE IV

Estimation of t* by Third Method

Parameter	Center frequency f_m, Hz						
	0.39	0.74	1.51	2.96	5.5	11.1	25.0
t_3, s, s	500	500	100	140	50	50	100
$\log \bar{a}_s$	1.24	1.07	1.82	2.53	2.94	3.22	3.57
$\log \bar{a}_c$	−1.39	−1.67	0	−0.67	1.03	1.19	0
t*, s	129	39	41	59	46	34	23
u	5.2	12.1	2.4	3.2	1.2	1.9	5.3

TABLE V

Estimates of Anisotropic Scattering

Parameter	Center frequency f_m, Hz		
	1.51	2.96	5.5
q, s^{-1}	0.0065	0.0058	0.0070
t_0, s	51	57	47
t_a^*, s	3.1	3.4	2.9
Λa	4.7	10.3	16

TABLE VI

Summary Estimates

Parameter	Center frequency f_m, Hz						
	0.39	0.74	1.51	2.96	5.5	11.1	25.0
t^*_{av}, s	97	41	43	55	42	26	19
t_Q, s	122	79	24	16.6	12.0	10.4	9.2
l, km	339	145	151	192	147	91	67
Λ	38	31	65	162	230	290	480

length 1. The Λ_a values are also given in Table V; they look physically reasonable. Obviously, these values should be regarded as tentative, but they can be used for general orientation.

Finally, the average t* values estimated by the three methods are listed in Table VI. They were obtained by the formal geometrical averaging of the data given in Tables I, III, and IV.

DISCUSSION OF THE RESULTS

The disagreement between the t* values estimated by method 1 and methods 2 and 3 is not great, being two-fold only at the 25 Hz channel, for which the results are in general relatively unreliable. As a whole, the agreement can be considered good.

The proximity of the estimates obtained from methods 2 and 3 is not representative. As we have mentioned above, almost in all cases we used the second equation of (7) which matches (11) for $t_d = t_s$. The question, therefore, arises as to what extent the t* estimates are independent in the case where Q values are obtained by adjustment of the same equations. We have not found a good solution to this problem. We should, obviously, consider the t* estimates by methods 2 and 3 as notably correlated. On the other hand, the fact that the coda asymptote can be well adjusted by the curve of (36) for u = 0.2–3 proves the validity of our initial model (7); its theoretical substantiation is not available for this interval.

The comparison of the t* and $t_Q = (2\pi f_m/Q)^{-1}$ values allowed us to estimate separately the attenuation and scattering effects beneath Kamchatka. We found that the two effects are comparable.

Table VI includes the values of $1 = \alpha^{-1} = ct^*$ and the dimentionless "scattering number" $\Lambda = 1/\lambda = t^* f_m$. Like the quality factor Q, the Λ value characterizes the intensity of scattering as a process and can be useful in comparing the results obtained in different frequency bands. (A similar quantity "transparency", equal to $\Lambda/2\pi$ in our notation, was proposed by A. B. Nikolayev [5]).

It should be noted that for the model with a self-similar spectrum of heterogeneities ($N(L) \sim L^{-3}$, $S(k) \sim k^3$, where L is the size of an individual heterogeneity and k is the wavenumber) the scattering number must be constant for any frequency f, and departures from this rule indicate that the spectrum of heterogeneities ceases to be self-similar. We see that Λ is relatively stable in the range of 0.3–1 Hz and increases with frequency by about one order of magnitude in the range of 1–30 Hz. This fact can be compared with the similar behavior of the seismic radiation spectrum from a strong earthquake. For the

considered frequencies this radiation is generated by near-surface heterogeneities of a seismogenic fault and branching ruptures, and if the spectrum of these heterogeneities is self-similar ($N(L) \sim L^{-2}$, $S(k) \sim k^2$), the acceleration spectrum should be constant like Λ. The behavior of the spectra of real accelerograms is actually different; they are roughly flat in the range of 0.5–3 Hz and have an explicit decay at 3–30 Hz which cannot be explained by anelastic attenuation. This analogy in the behaviors of the spectra of heterogeneities in the earth revealed by two different types of initial data seems remarkable.

The study of anisotropic scattering seems to corroborate our initial hypothesis of a strong scattering effect at reflectors. The estimates of the isotropization time t_0 are close to the t^* values for the same channels. Since the t^* and, especially, t_0 data are of low accuracy, we cannot say with certainty that the effect of isotropic scattering proper is insignificant, but we can definitely state that multiple anisotropic scattering makes a significant contribution to the observed wave field.

It should be noted that our statistical method of describing the variation in the shape of a short-period seismic pulse with distance is complementary to the description of this phenomenon by ray-tracing in a multilayered earth. This description seems to be advantageous when applied to laterally heterogeneous "block-type" media.

Comparison of our results with those from other regions of the USSR would be of great interest, but owing to the differences in the technique such comparison is reasonable only in one case. Kopnichev [3] estimated α and 1 for the crust in the northern part of the Garm region in Tajikistan using a similar technique. His 1 estimates for $f = 5$ and 10 Hz were 100 and 50 km, which differ little from the estimates we obtained for the crust and upper mantle under Kamchatka (147 and 91 km, respectively).

CONCLUSION

1. It is suggested that the diffusion approximation formula be applied to the intensity of scattered waves in the region intermediate between the Born and diffusion cases.
2. Three methods of estimating the scattering characteristics of the crust and upper mantle were applied beneath Kamchatka in the frequency band of 0.3–30 Hz. The estimates obtained are in good agreement.
3. Anisotropic scattering characteristics are estimated; it is shown that multiple anisotropic scattering is an important and, possibly, the determining factor in the general pattern of diffusion.

REFERENCES

1. S. A. Boldyrev, in: *Seĭsmichnost', seĭsmicheskiĭ prognoz, svoĭstva verkhneĭ mantii i ikh sviaz' s vulkanizmom na Kamchatke* (Seismicity, earthquake prediction, upper mantle properties, and their relation to volcanism in Kamchatka) (Novosibirsk: Nauka. 1974): 200–213 (in Russian).
2. A. A. Gusev and V. K. Lemzikov, *Vulkanol. i Seĭsmol.* No. 6: 82–93 (1980) (in Russian).
3. Yu. F. Kopnichev, *Dokl. AN SSSR* 255, No. 2: 305–309 (1981) (in Russian).
4. Yu F. Kopnichev, *Seĭsmicheskiye koda-volny* (Seismic coda waves) (Moscow: Nauka, 1978) (in Russian).
5. A. V. Nikolayev, *Seĭsmika mutnykh i neodnorodnykh sred* (Seismics of turbid and heterogeneous media) (Moscow: Nauka, 1973) (in Russian).
6. V. V. Ol'shevskiĭ, *Statisticheskiye svoĭstva morskoĭ reverberatsii* (Statistical properties of marine reverberation) (Moscow: Nauka, 1966) (in Russian).
7. T. G. Rautian, V. I. Khalturin, M. S. Zakirov et al., *Eksperimental'nye issledovaniya seĭsmich-*

eskoĭ kody (Experimental study of seismic coda) (Moscow: Nauka, 1981) (in Russian).
8. S. M. Rytov, *Vvedeniye v statisticheskuyu radiofiziku* (Introduction to statistical radiophysics) (Moscow: Nauka, 1966) (in Russian).
9. K. Aki and B. Chouet, *J. Geophys. Res.* 80, No. 23: 3322–3342 (1975).